The 12-pulse multi-level rectifier: commutation aspects, design of the reactors and control strategy

Yeddo B. Blauth
Universidade Federal do Rio Grande do Sul
Departamento de Engenharia Elétrica
e-mail: yeddo@inep.ufsc.br
fone: (048) 234-3127
fax: (048) 234-5422

Ivo Barbi
Universidade Federal de Santa Catarina
Instituto de Eletrônica de Potência - INEP
e-mail: ivo@inep.ufsc.br
fone: (048) 331-9204
fax: (048) 234-5422

***Abstract* - This paper presents important new points about the 12-pulse multi-level rectifier, which is a suitable choice for high power factor (PF) high power rectifiers. In the introduction, a brief review of the circuit operation is presented. Along the text, the commutation phenomena are analyzed, the influence of the reactor inductances in both the input current and the power factor is presented to help the design of the reactors. A control system capable of guaranteeing the output voltage stability, a good transient response and the equality of the reactor currents is also presented and analyzed. Experimental results of a 5kW prototype are given to confirm the developed theory.**

I. Nomenclature

fi - Cut off frequency of the current control inner loop.
fv - Cut off frequency of the voltage control loop.
V_{CM} - Control voltage maximum value, usually 5V or 10V.
V_L - Line voltage.

II. Introduction

According to previous studies, the 12-pulse multi-level rectifier is a suitable choice for high power rectifiers because it has a unity displacement factor (DF), a high PF, low losses and low total harmonic distortion (THD) of the input current [1,2]. Equations of the output voltage and the input current, as well as the open loop analysis can be found in those studies.

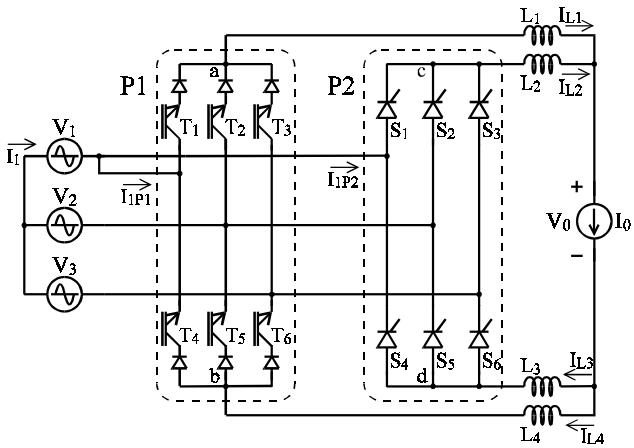

Fig. 1. Proposed rectifier circuit configuration.

The proposed rectifier is shown in Fig. 1. The circuit is composed by two three-phase 6-pulse rectifiers P1 and P2 connected in parallel by four equal balancing reactors L_1 - L_4. P2 is a conventional thyristor rectifier with a lagged firing angle α and P1 is composed by GTOs or IGBTs and diodes, operating with a led and symmetrical firing angle -α.

The adopted modulation strategy is shown in Fig. 2.

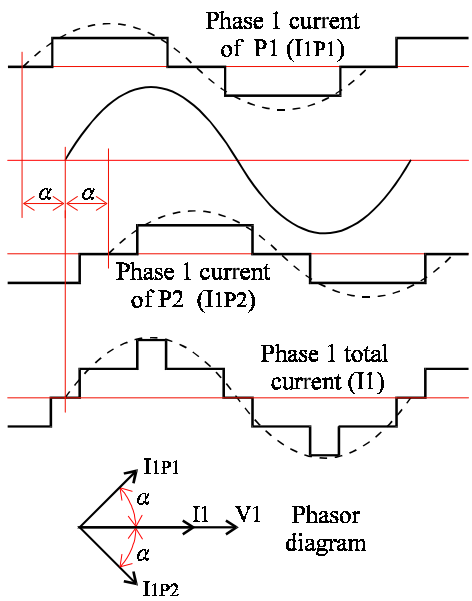

Fig. 2. Proposed rectifier modulation strategy.

The phase voltage V_1 and the currents I_{1P1}, I_{1P2} and I_1 that appear in Fig. 2 are defined in Fig. 1.

The phasor diagram clearly shows that the first harmonic of the total input current I_1 and the phase voltage V_1 are in phase. Therefore, the DF is unitary for any firing angle α. Fig. 2 also shows that the total input current has a complex waveform and how multi-level current is achieved.

III. The commutation phenomena

Fig. 3 shows the reactive components L and C that help the proposed rectifier commutation process.

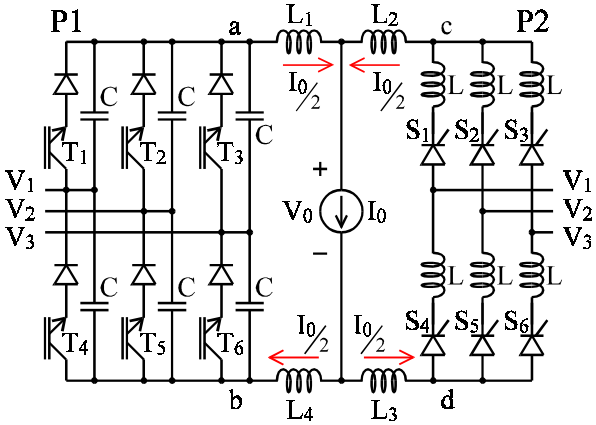

Fig. 3. Commutation reactive components L and C.

From Fig. 3 it can be noticed that the output current of both P1 and P2 rectifiers are considered as half of the output current I_0 and, therefore, the 12-pulse rectifier is being assumed as perfectly balanced, with the desired equality among the currents of the reactors.

Line or intentionally placed inductances cause a well-known commutation process in thyristors rectifiers like P2 [3,4]. These commutations are responsible for overlap periods when two thyristors (e.g. S_1 and S_2) are conducting simultaneously and both the input current and the output voltage change from their ideal waveforms. These overlap periods can be calculated by (1).

$$\mu_L = \text{Arc}\cos\left(\cos\alpha - \frac{\omega\, L I_0}{\sqrt{2}\, V_L}\right) - \alpha \qquad (1)$$

The output voltage of P2 is given by (2).

$$V_{cd} = \frac{3\sqrt{2}\, V_L}{\pi}\cos(\alpha) - \frac{3\omega L I_0}{2\pi} \qquad (2)$$

On the other hand, the commutation process in rectifiers like P1 is completely different and its analysis is not easily found in the literature. For this reason, the step by step P1 commutation process is presented in Fig. 4.

Assuming that T_1 and T_5 were conducting (Fig. 4a), the commutation process begins when T_5 is turned off and the gate signal of T_6 becomes positive. The commutation happens without currents in the involved switches (e.g. T_5 and T_6), according to Fig. 4(b). The load current of P1, which is half of the proposed rectifier load current, distribute itself among C_4, C_5 and C_6. Assuming these capacitances are equal, each capacitance will conduct the third part of the P1 load current. The currents of the lines 2 and 3 will become equal to $-I_0/6$ and the current of the line 1 will become equal to $I_0/3$. When the voltage across capacitance C_6 become equal to zero, T_6 starts conducting and the commutation process ends (Fig. 4c).

The remarkable waveforms of P1 considering the commutation phenomena are shown in Fig. 5.

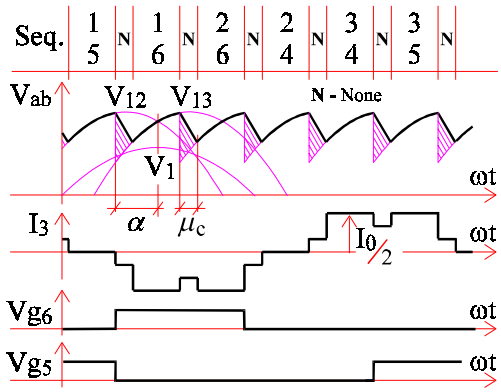

Fig. 5. Waveforms of P1 considering the commutation phenomena. From top to bottom: Conducting sequence (the numbers in the line "seq." are the numbers of the conducting switches), output voltage V_{ab} (including phase voltage V_1, line voltages V_{12} and V_{13}, and dashed zones denoting the output voltage increase due to the commutation), line current I_3, and T_6 and T_5 firing pulses.

From Fig. 5 it can be noticed that as in the thyristor rectifier, both the input current and the output voltage also change from their ideal waveforms in the P1 rectifier. Fig. 5 also shows which switches are conducting at every time (line "seq."), given all the needed information to design the firing pulses.

From the analysis of Figs. 4 and 5 the equations of the output voltage Vab and the commutation period μ_C can be developed, according to (3) and (4).

$$\mu_C = \frac{2\sqrt{6}\,\omega C V_L}{I_0}\left[\text{sen}\left(\alpha + \frac{\pi}{6}\right) + \text{sen}\left(\alpha - \frac{\pi}{6} - \mu_C\right)\right] \qquad (3)$$

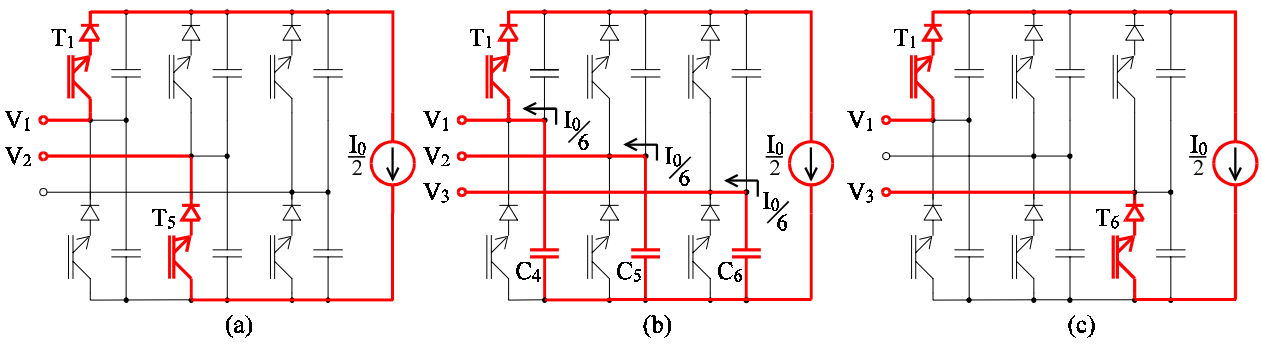

Fig. 4. Step by step P1 commutation process.

$$V_{ab} \approx \frac{3\sqrt{2}V_L}{\pi}\left[\cos(\alpha) + \frac{\mu_C}{2}\operatorname{sen}(\alpha)\right] \quad (4)$$

From (2) and (4) it can be seen that both equations have the same term with "cos(α)", which gives the average output voltage without considering the commutation phenomena, and one more term, which appears due to the commutation. This second term is negative in (2) and positive in (4). Therefore, the commutation phenomena increase the unbalance among the currents of the reactors, because they increase the output voltage of P1 and they decrease the output voltage of P2.

It is interesting to notice that while the inductances in P2 limit their di/dt and cause a lossless zero current switching (zcs) in all commutations of all thyristors, the capacitances in P1 limit their dV/dt and also cause lossless commutations, but of the zero voltage switching (zvs) type. Therefore, the 12-pulse multi-level rectifier has not switching losses and the switches stress can be kept under specified values.

The design of the commutation reactive components can be made as functions of the maximum allowable derivatives of the switches, according to (5) and (6).

$$C \cong \frac{I_0}{6\left|\frac{dV}{dt}\right|_{MAX}} \quad (5)$$

$$L \cong \frac{\sqrt{2}V_L}{2\left|\frac{dI}{dt}\right|_{MAX}} \quad (6)$$

IV. The Design of the Reactors

Fig. 6 shows the voltages and the currents of the reactors L_1 and L_2.

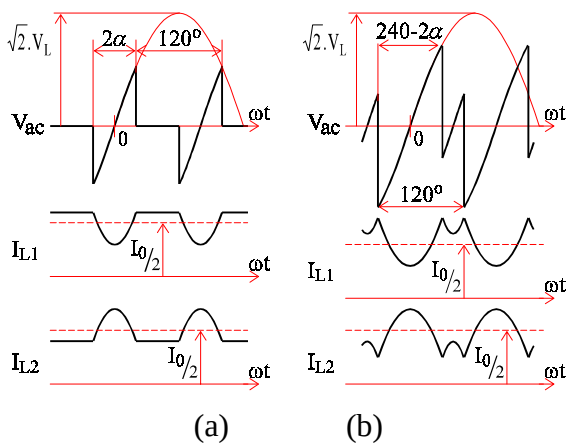

Fig. 6. Voltages and currents of the reactors L_1 and L_2. (a) $0^o \le \alpha \le 60^o$. (b) $60^o \le \alpha \le 90^o$.

From Fig. 6 and some algebraic calculations, it can be concluded that, to guarantee continuous conduction it is enough satisfying (7) and (8) when $0^o \le \alpha \le 60^o$, and satisfying (7) and (9) when $60^o \le \alpha \le 90^o$.

$$Ln > \sqrt{2} + \left(\frac{3\sqrt{2}.\alpha}{\pi} - \sqrt{2}\right)\cos\alpha - \frac{3\sqrt{2}.\operatorname{sen}\alpha}{\pi} \quad (7)$$

$$Ln > \frac{3\sqrt{2}}{\pi}\left(\operatorname{sen}\alpha - \alpha.\cos\alpha\right) \quad (8)$$

$$Ln > \frac{3\sqrt{2}}{\pi}\left[\left(1 - \frac{\pi\sqrt{3}}{6}\right)\operatorname{sen}\alpha + \left(\frac{\pi}{2} - \alpha\right)\cos\alpha\right] \quad (9)$$

In the above inequalities (7, 8 and 9) the term in the left side Ln is called the normalized inductance and is defined according to (10).

$$Ln = \frac{I_0.\omega.L}{V_L} \quad (10)$$

Figure 7 shows the above inequalities (7, 8 and 9).

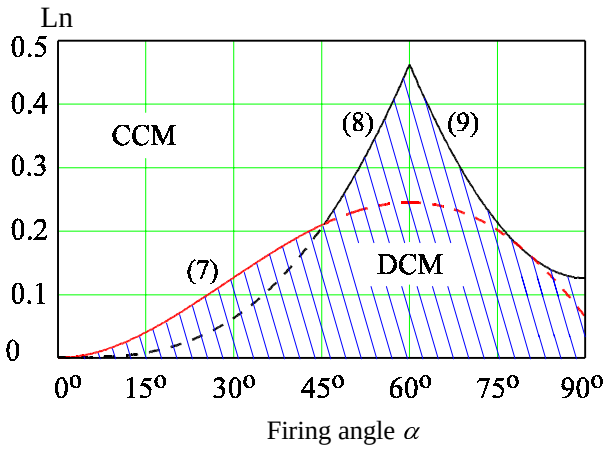

Fig. 7. Normalized inductance of the balancing reactors that causes continuous conduction as a function of the firing angle α.

From Fig. 7 it can be concluded that, if continuous conduction is expected and α is smaller than approximately $45{,}5^o$ it is enough satisfying (7). Otherwise, it is enough satisfying (8) or (9). From Fig. 4 it can also be concluded that the less favorable case is when $\alpha = 60^o$. In this case the critical normalized inductance is approximately 0.46. For this reason, the critical inductance Lc is defined according to (11).

$$Lc \approx 0.4624\frac{V_L}{\omega I_0} \quad (11)$$

Including the ripple of the reactors current shown in Fig. 6 in the ideal waveform of the input current of Fig. 2 leads to the real input current and allows exact calculations. Assuming a constant current load, it can be shown from these calculations that the normalized RMS current of the reactor L_1 (I_{L1}/I_0), the PF and the THD of the input current of the 12-pulse multi-level rectifier are those presented in Figs. 8, 9 and 10.

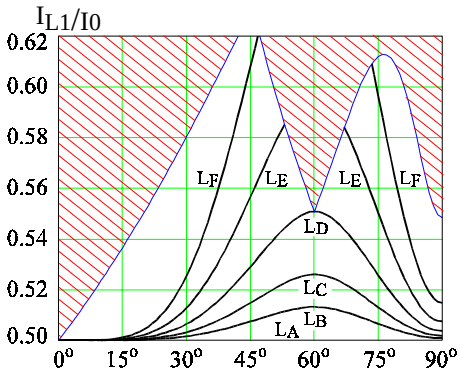

Fig. 8. Normalized RMS currents of the reactors

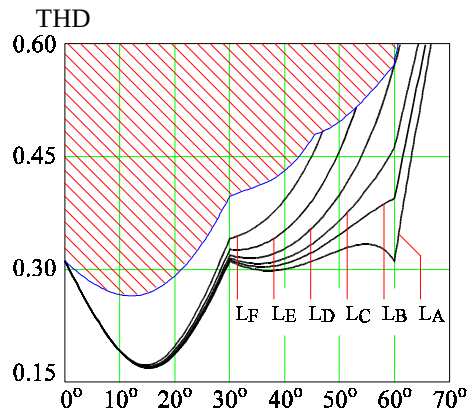

Fig. 9. THD of the input current.

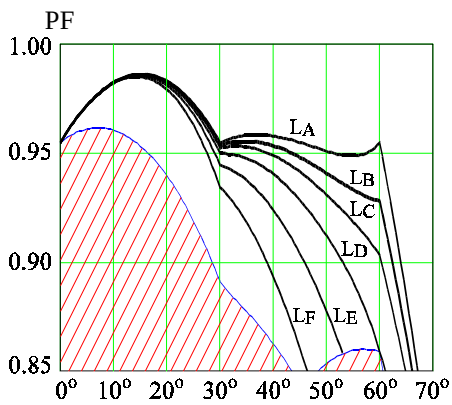

Fig. 10. Power Factor of the 12-pulse rectifier.

The dashed zones in Figs. 8, 9 and 10 denote zones where the conduction of the reactors are discontinuous. Figures 8, 9 and 10 show functions of the firing angle α and are plotted only to the following values of the reactor inductances:

$$L_A \approx \infty \text{ (ideal)} \qquad L_B = 2.Lc$$

$$L_C = \sqrt{2}.Lc \qquad L_D = Lc$$

$$L_E = \frac{Lc}{\sqrt{2}} \qquad L_F = \frac{Lc}{2}$$

The RMS current of the balancing reactors L_1, L_2, L_3 and L_4 are equal. Therefore, Fig. 8 gives any of them.

From Figs. 9 and 10 it can be concluded that the THD and the PF do not change much with the reactors inductances when $0^o \le \alpha \le 30^o$. Therefore, small reactors can be used if the rectifier is primarily intended to operate in this band.

On the other hand, if large variations of the output voltage are necessary, the reactor inductance choice must be done according to the expected overall performance of the rectifier.

As an example, if the rectifier operates with $\alpha \le 60^o$ and the PF must to be always larger than 0.90, then the inductance of the reactors must be larger than the critical inductance (Fig. 10) and the wires of the reactors must be designed to a RMS current of 0.55 I_0 (Fig. 8).

V. The Closed Loop Analysis

To guarantee a perfect current sharing among reactors it is advisable to use a control system, because small variations in the firing angle or in any other internal parameter of the rectifier can cause large variations of any of the four reactor currents [1,2]. Therefore, the best choice is to control all four currents independently. However, controlling only one current of each bridge, e.g. I_{L1} and I_{L2} (Fig. 1), can also give good results, because differences between bridges are much larger than internal differences into one bridge. The followed developed theory is based on this idea.

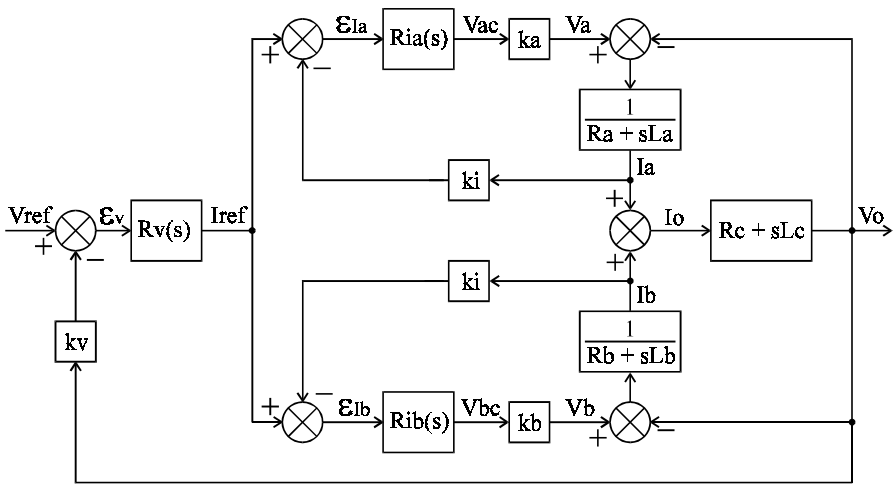

Fig. 11. Block diagram of the control system.

Fig. 11 shows the block diagram of the adopted control system. Va and Vb are the output voltage of the bridges P1 and P2, Ra and Rb are the internal resistances of the bridges P1 and P2, La = Lb = $2L_1 = 2L_2$, Rc and Lc are the LR load series equivalent, Ia and Ib are the reactors currents I_{L1} and I_{L2} that must be controlled, I_0 and V_0 are the rectifier output current and voltage. Fig. 7 also shows the output voltage controller Rv(s) and the current controllers Ria(s) and Rib(s). V_{ab} and V_{bc} are P1 and P2 control voltages, kv and ki are the gains of the output voltage and current transducers. ka and kb are linear approximations of the bridges gains, according to (12).

$$ka = kb = \frac{3\sqrt{2}}{\pi} \cdot \frac{V_L}{V_{CM}} \tag{12}$$

In order to achieve single pole closed loop transfer functions, the design of the controllers can be made according to (13 - 15):

$$Ria(s) = \frac{2\pi fi.(Ra + 2Rc)}{s.ka.ki}\left(1 + s\frac{La + 2Lc}{Ra + 2Rc}\right) \tag{13}$$

$$Rib(s) = \frac{2\pi fi.(Rb + 2Rc)}{s.kb.ki}\left(1 + s\frac{Lb + 2Lc}{Rb + 2Rc}\right) \tag{14}$$

$$Rv(s) = \frac{\pi ki.fv\left(1 + s\frac{1}{2\pi fi}\right)}{s.kv.Rc\left(1 + s\frac{Lc}{Rc}\right)} \tag{15}$$

VI. Experimental Results

In order to verify the developed theory a 500Vdc, 5kW prototype was built. The controllers were designed according to (13), (14) and (15). The adopted cut off frequencies were fi = 5Hz and fv = 3Hz, with theoretical time constants of τ_I = 31.8ms and τ_V = 53.1ms.

Figures 12 and 13 show experimental results of both the current control inner loop (Fig. 12) and the voltage control loop (Fig. 13).

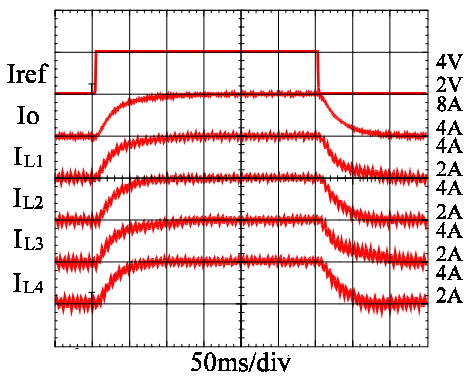

Fig. 12. Experimental results of the 5kW prototype current control inner loop.

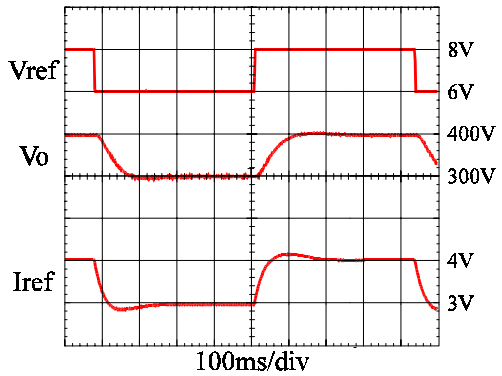

Fig. 13. Experimental results of the 5kW prototype voltage control loop.

From Fig. 12 it can be observed that all reactor currents have the same steady state, although small differences can be seen in the transient response of the non-controlled currents I_{L3} and I_{L4}. The expected equality among the reactor currents was reached and, therefore, the rectifier works with the best overall performance that is possible considering the chosen reactor inductances. Fig. 12 shows that the output current I_0 has the expected single pole transient response with an associate time constant of about 30ms and Fig. 13 shows that the output voltage Vo also has a single pole transient response, but with an associate time constant of about 50ms. Finally, from the transient response presented in Figs. 12 and 13 it can be concluded that the system has very good stability, confirming the efficiency of the implemented control system.

VII. Conclusion

In this work, important new points about the 12-pulse multi-level rectifier were presented. It was shown that the commutation phenomena don't cause additional losses and increase the unbalance among the reactor currents. General conditions to reach continuous conduction were developed and it was shown that the less favorable case is when α = 60º. The influence of the reactor current ripple on the performance parameters was analyzed and it was shown that THD and PF do not change much with reactor inductances when $0º \leq \alpha \leq 30º$. Therefore, small reactors can be used if the rectifier is primarily intended to operate in this band. A control system capable of guaranteeing the equality among the reactor currents and a good system stability was presented. The system was implemented and valuable experimental results can be observed.

VIII. References

[1] Y.Blauth and I.Barbi, "A Phase-Controlled 12-Pulse Rectifier with Unity Displacement Factor without Phase Shifting Transformer", *Conference Proceedings of the APEC'98*, pp. 970 - 976.

[2] Y.Blauth and I.Barbi, "A New Three Phase Rectifier with Unity Displacement Factor and Current Multilevels", *Conference Proceedings of the COBEP'97*, pp. 396 - 401.

[3] B.R.Pelly, "Thyristor Phase-Controlled Converters and Cycloconverters," *New York: Wiley Interscience*, 1971.

[4] I.Barbi, "Eletrônica de Potência", *Editora da UFSC*, 1986.